ISSN 1729–5106

EAST AFRICAN JOURNAL OF PHYSICAL SCIENCES

Volume 6 — Part 2 December 2005

Contents

An International Journal of Pure and Applied Science

East African Journal of Physical Sciences 6(2): 89–100 (2005)

Gravity Survey of Lake Magadi Area

J.G. Githiri[1*], J.W. Waithaka[2], J. Okumu[2], R.L. Stangl[2]
[1] Physics Department, Jomo Kenyatta University of Agriculture & Technology,
P.O. Box 62000 - 00200, Nairobi, Kenya
[2]Kenyatta University, Physics Department, School of Pure and Applied Sciences,
P.O. Box 43844 - 00100, Nairobi, Kenya
*corresponding author, E-mail: jggithiri@yahoo.com

A gravity survey was conducted in the area surrounding Lake Magadi to investigate presence of any geological bodies related to high heat flow in the area. Gravity stations were established by filling up the unsurveyed sectors in a previous Leicester gravity study. Gravity data collected in the area was subjected to necessary corrections and a Bouguer anomaly map drawn. The Bouguer gravity values were found to range from –1800 to –1680 gu with the maximum peak occurring at the NNE part of the project area. Forward modeling along selected profiles p-q, m-n, c-d and h-g was done. Depths to the top of bodies pq, mn, cd and hg were found to be 0.2-0.7, 0.15, 0.5, and 0.04 km, while depths to the bottom were modeled as 4.0, 6.0, 4.0 and 3.6 km, respectively. The bodies have density contrasts ranging from 280-340 kg/m^{3}, and were modeled as dike like structures elongated in N-S and NNW-SSE directions. This direction is nearly the characteristic trend of tectonic structures in the rift valley. A model where the dikes originate from a shallow magma chamber is proposed.
Key words: gravity, anomalies, Magadi, survey.

INTRODUCTION

Magadi is located in the Southern part of the Kenyan Rift valley, an active continental rift. This part of the rift is characterised by intense faulting and abnormally high heat flow (Baker, 1958). The present day activity in Magadi area include extensive seismicity with presence of earthquake swarms in the area north of lake Magadi (Seht *et al.*, 2001). Like the Olkaria-Longonot-Suswa region which are currently productive geothermal fields with fumarolic vents, Magadi area has widespread hot springs distributed along the shores of lake Magadi. Leicester gravity survey conducted over the whole of Kenya by Khan *et al.* (1977), detected gravity highs, the most prominent representing volcanoes along the rift valley. Two isolated gravity highs were also detected in the Magadi area. This study was conducted for the purpose of investigating the presence of any geological bodies with sufficient density contrast which may be the cause of high heat flow and presence of hot springs in the area around Lake Magadi.

Location and Tectonics

The study area shown in Figure 1 situated in the Magadi trough is bounded by latitude -1°48', -2°01' and longitudes 36°15', 36°24', respectively comprising an area of about 241 square kilometers. The area has experienced extensional tectonics, normal rifting and voluminous eruptions of alkaline volcanic rocks since Miocene time. Relative high upper crust temperatures and heat flow occur along the rift, associated with crustal thinning and the presence of shallow magma chambers (Ndolo, 1989). Thermal manifestations in form of hot springs are evident distributed along the shores of Lake Magadi.

The geology of the area is as a result of volcanism and a tectonic activity of the rift. The area is largely covered by Quaternary sediments, which overlie extensive pleistocene trachyte

 ISSN 1729–5106

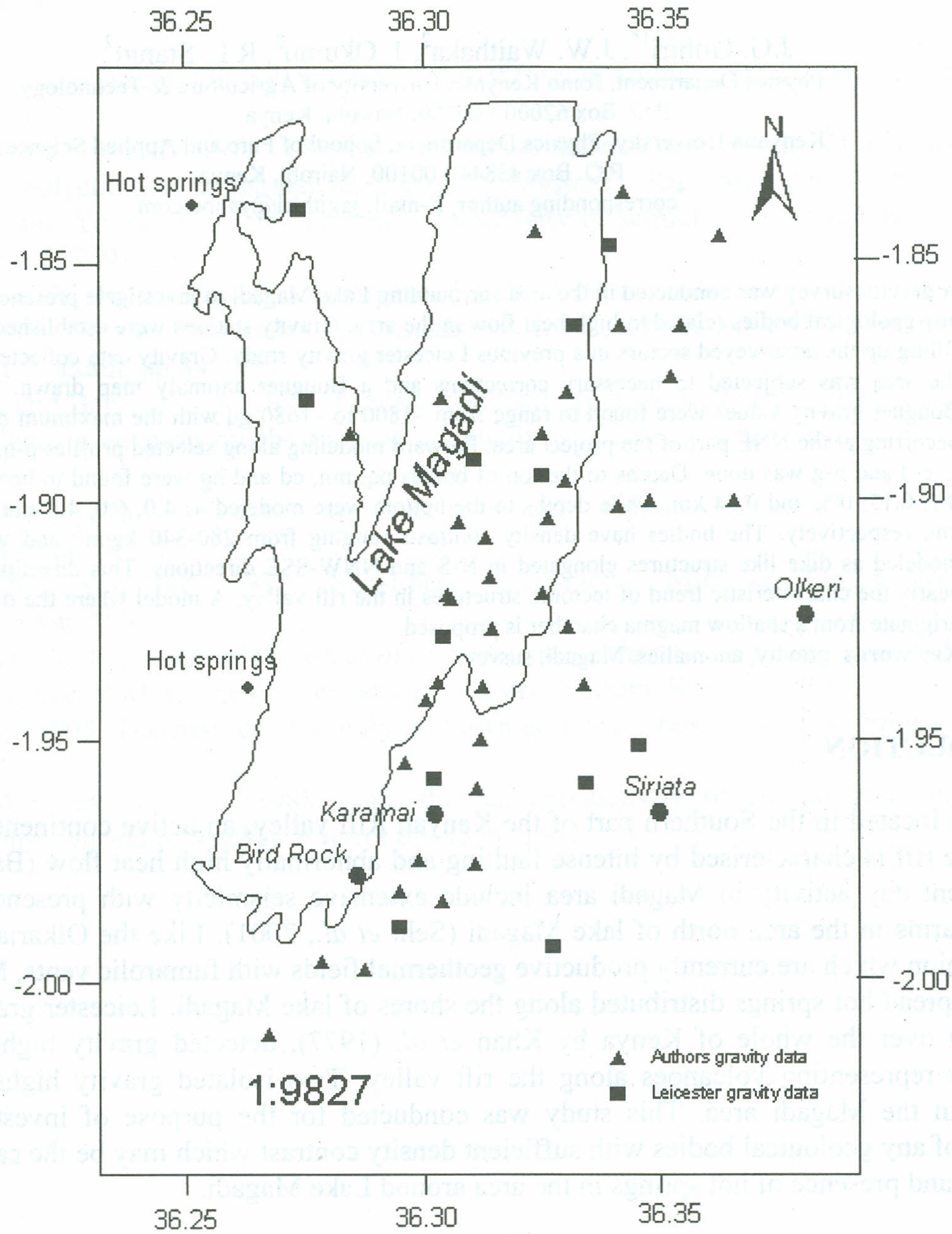

Figure 1: Study area with gravity stations.

lavas. The trachyte lava overlies extensive basalts and nephelinites, which in turn rest on gneisses and schists of an archean basement system. The regional tectonic pattern of this sector of the rift valley has mainly north- south directional trend, which is related to the several stages of rifting process. Muiruri (1992) indicated that the north–south trending normal faults affects miocene and pliocene volcanics on the rift shoulders but there are smaller, younger and closely spaced north-south faults that cut the most recent volcanics between Suswa area and lake Magadi.

The Magadi area covers a greater part of the width of the Rift Valley and it includes the Western boundary faults. The floor of the valley descends with many steps due to the escarpments, from East to West down the deepest trough, which is central in the area occupied in its most southern part by Lake Magadi as explained by Baker (1958). A dense network of grid faults that belong to the rift floor faults affects the area. These faults especially the North-South trending faults control occurrence of the geothermal manifestations as indicated by Riaroh & Okoth (1994).

Field Measurements

A total of 45 stations were established at an average spacing of 1 km and positioned using a Global Positioning System (GPS) model Garmin 45. The stations were established near roads and motorable tracks for easy accessibility. Regular grid separation of the stations was impossible due to rains that had made most of the lower areas surrounding the lake to flood. The station distribution is as shown in Figure 1.

Station heights were extrapolated from the topographic map of the study area sheet number 160/4 of scale 1; 50,000 published by survey of Kenya. The gravity measurements were carried out using a Worden gravimeter model prospector W.S 410. Other data sets from 12 stations by Khan *et al.* (1977) were integrated in the study with eight of them being preoccupied to harmonize all the gravity measurements. The average difference of gravity values at the preoccupied station as compared to the previous survey data was added to all the other acquired data sets for harmonization.

Data Processing

Bouguer anomaly is usually obtained by subtracting the predicted value from the observed value of gravity. The observed value is achieved by removing the effects of tides and the instrumental drift from the raw gravity measured value in the field. The predicted gravity value is the theoretical gravity at the reference ellipsoid corresponding to the latitude of the station after carrying out of the free-air, Bouguer and terrain corrections. The Bouguer anomaly will be the contribution on gravity due to crustal and upper mantle variations in density.

The tidal corrections were determined using a software GTIDES, (R.Stangl, Personal communication) and added to the raw data to allow performing of drift corrections. Figure 2 shows a tidal curve monitored at a station 1.97° S, 36.28° E. Repeated gravity readings at the base station were recorded daily with a periodicity of at most 3 hours for drift correction. The drift corrections obtained were relatively small not exceeding 3.0 gu. Figure 3 shows a drift curve monitored using station A23 as the base station. All the gravity measurements were referred to a local datum base station with a gravity value of 9777412 gu after carrying out tidal and instrumental drift corrections. The precision of the gravity measurements was ±0.1 gu. From the merged data sets, the complete Bouguer anomaly was obtained after carrying out the

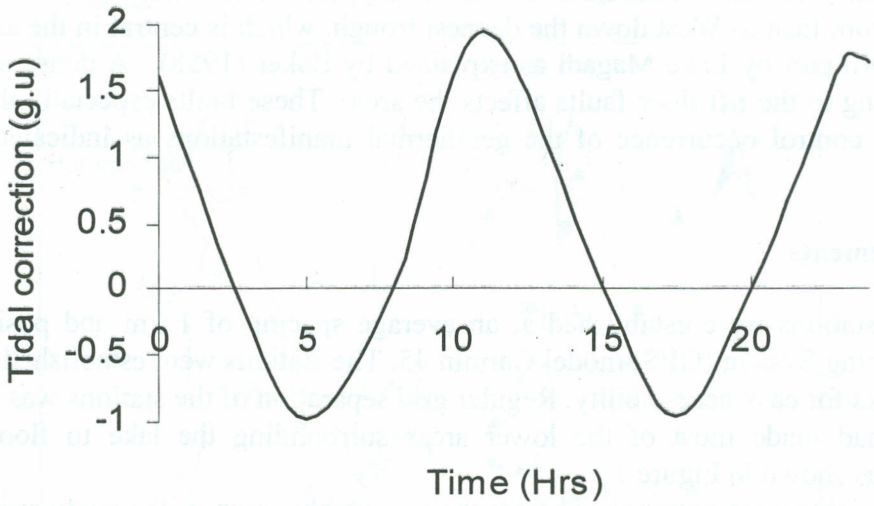

Figure 2: Tidal curve monitored at station 1.97ºS, 36.28ºE.

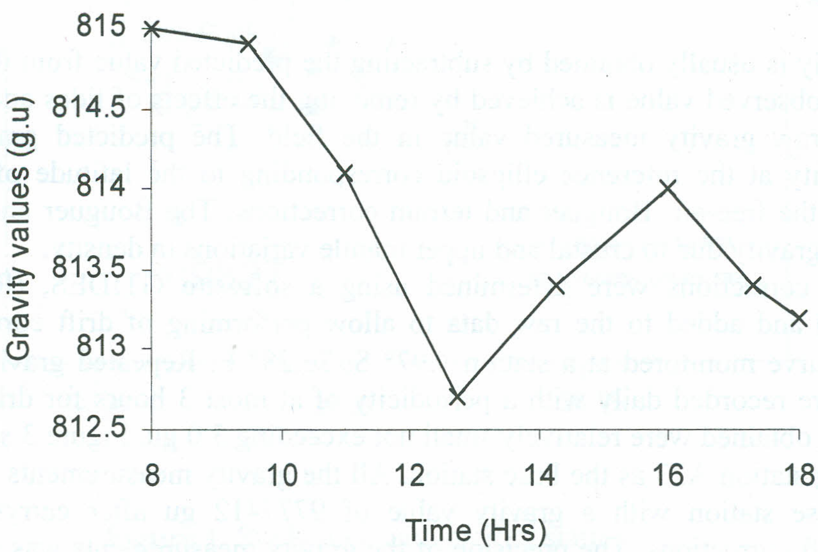

Figure 3: Drift curve monitored at base station A23.

latitude, free-air and Bouguer corrections to the observed gravity and subtracting the 1967 reference spheroid theoretical gravity value for the station location as in equation below.

$$g = 9780138.5\ (1 + 0.05278895 \sin^2\phi + 0.000023462 \sin^4\phi)\ \text{gu}$$

Where ϕ is the latitude angle of the gravity station in decimal degrees. A correction of (0.3086) gu per metre was used for the free-air correction and a function ($0.4191 * h * \rho$) for the Bouguer slab correction where h is the station height and ρ is the density of material between the datum level and the field station. Terrain effects were corrected for using a hammer chart with a maximum radius of 5 km. A Bouguer anomaly contour map of interval 5 gu was computed as shown in Figure 4, with a minimum of –1800 gu and a maximum of –1680 gu. Profiles were selected through the discerned anomalies in the Bouguer anomaly map. Isolation of the residual anomalies was done by removing the regional effects from the anomalies using graphical method along the selected profiles.

Empirical Depth Estimation

Quantitative interpretation involved direct calculation of values and the comparison of these values with those that were observed. Before attempting to fit calculated values to the observed anomaly, the depth estimates to the top of the bodies were empirically determined. The maximum depth rule (Kearey & Brooks, 1984) was used which calculates depth regardless of anomalous mass distribution. The depth rule states that if the maximum anomaly amplitude and the maximum horizontal gradient are A_{max} and A'_{max}, then the depth to the top of the body (z) is given by:

$$Z \leq 0.86\ A_{max} / A'_{max}$$

Results of limiting depths to the top of anomalies pq, mn, cd and hg obtained using maximum depth rule were 0.95, 0.86, 0.93 and 0.73 km, respectively.

Forward Modeling

In Forward modeling, an initial model for the source body is constructed based on prior geological and geophysical knowledge of the study area. The models anomaly is calculated and compared with the observed anomaly. The model parameters are adjusted to improve the fit between the observed and the calculated anomaly. The three-step process of body adjustment, anomaly calculation and comparison is repeated until both the calculated and observed anomaly curves achieve a 'best fit'. Due to non-uniqueness in gravity interpretation, prior geophysical and geological information are used as controls to the final models.

Forward 2-D modeling was done along profiles pq, mn, cd and hg using software based on algorithm by Talwani *et al.* (1959). In this method, the 2-D arbitrary body is assumed to have an infinite strike length. A body is approximated by polygons whose gravity effects are summed by numerical integration using an algorithm. During the modeling process, a 2 layer stratigraphic column was considered. The layers were assumed to be perfectly horizontal. The density of 2670 kg/m^3 was used for bottom and surface layers respectively. The limiting depths to top of the bodies obtained using the maximum depth rule were used in the start model during modeling process for each profile.

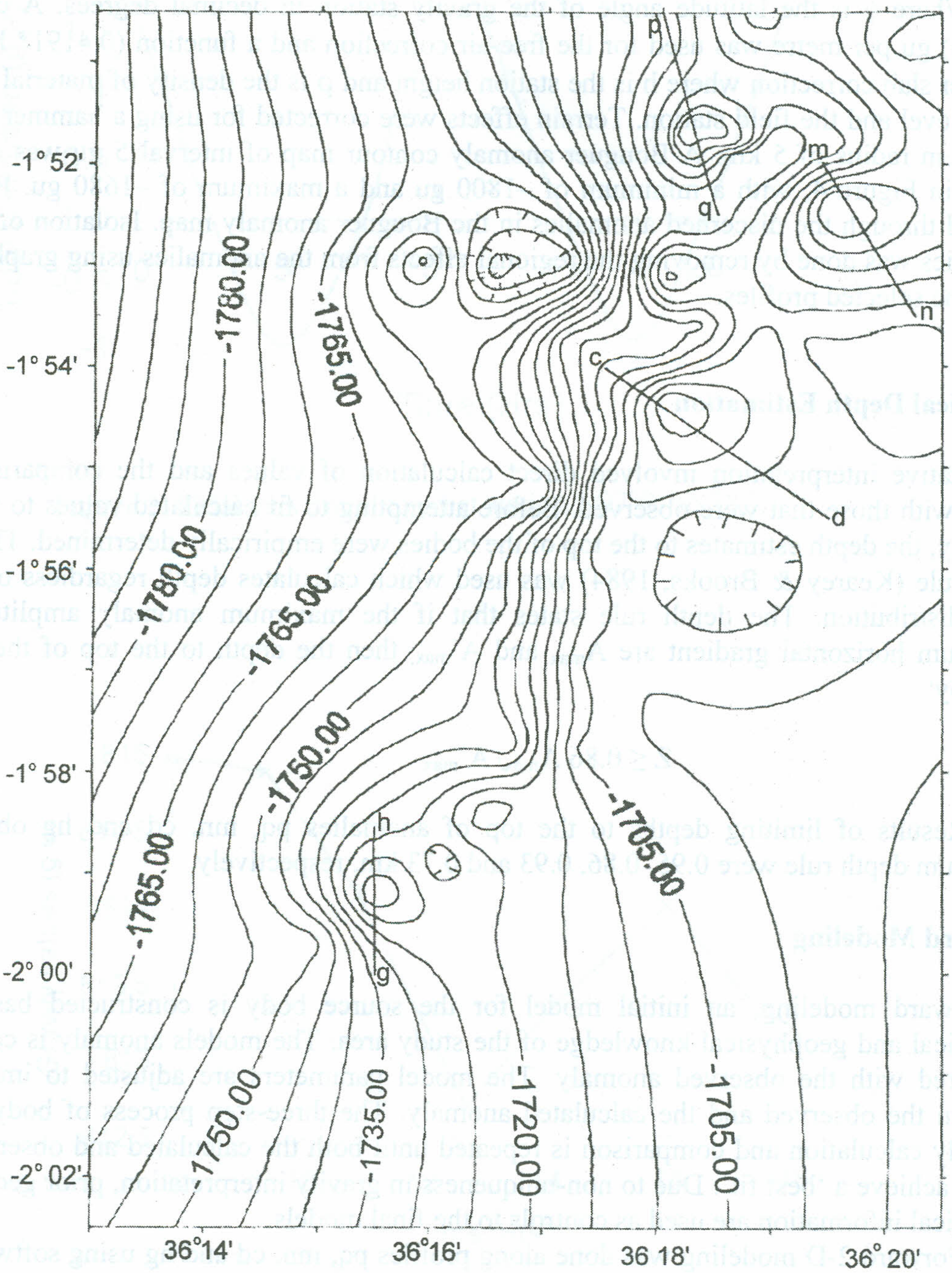

Figure 4: Bouguer anomaly map of study area (contour interval 5 gu).

RESULTS AND DISCUSSION

Profile p-q is oriented in NNW-SSE direction running normal to the strike of the anomaly. The causative structure is modeled as a composite of two bodies with positive density contrasts 280 kg/m^3 and 290 kg/m^3 respectively, the lower part having the highest density contrast. The width of the intrusive ranges from 0.4 to 0.6 km. The depth to the top of the body varies from 0.2 km to 0.7 km while its depth extent is up to 4 km. The results of modeling the anomaly p-q are shown in Figure 5a.

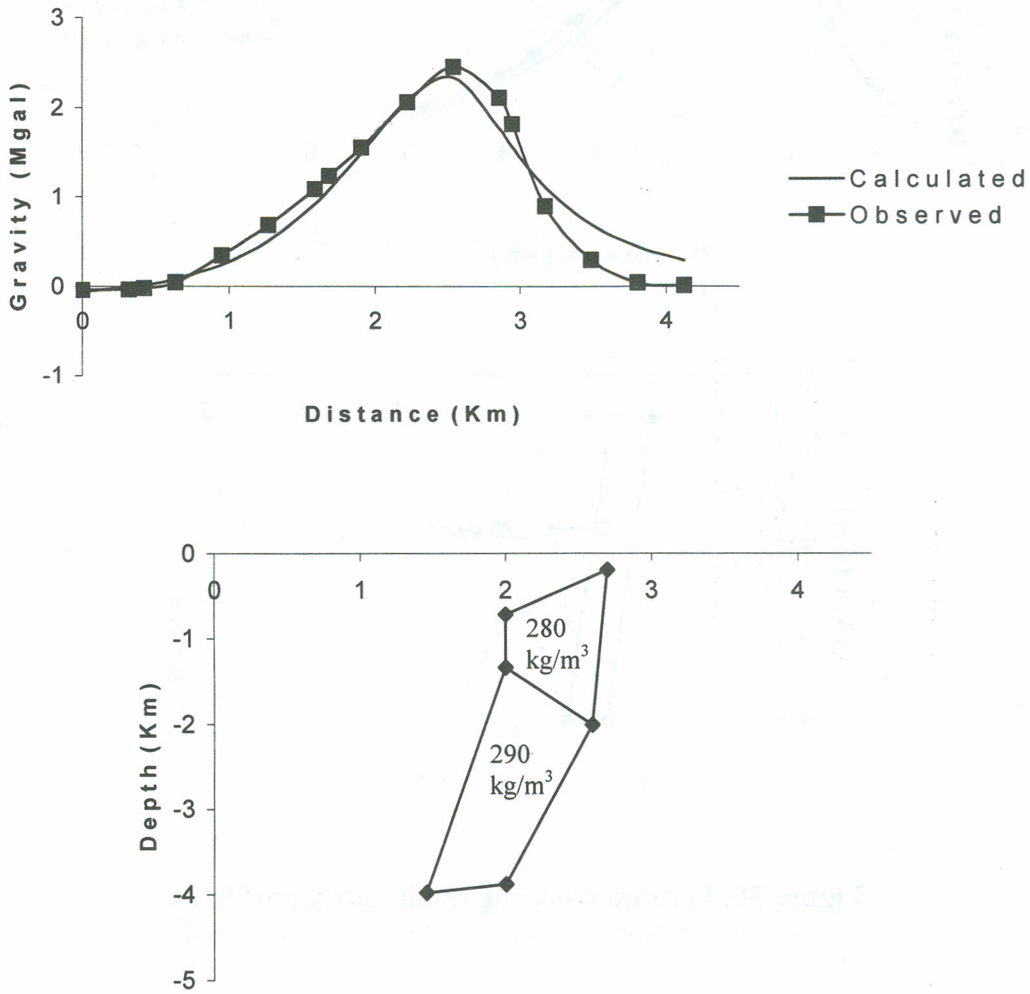

Figure 5a: Forward modeling results along profile p-q.

The profile c-d runs in NW-SE direction. The causative body modeled has a density contrast of 280 kg/m^3. The depth to its top is 0.5 km and it dips at an angle of 60° to the horizontal in approximately NW-SE direction. The depth to its bottom is 4 km. The results of modeling the anomaly c-d are shown in Figure 5b.

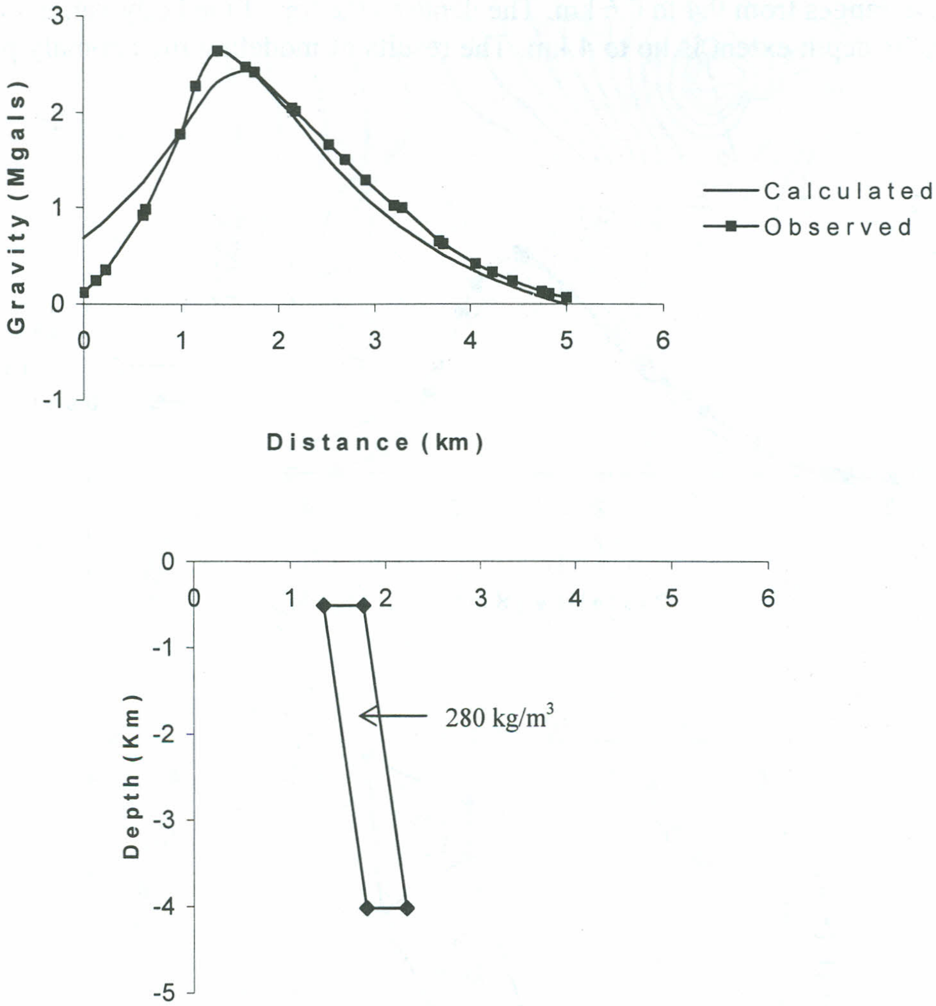

Figure 5b: Forward modeling results along profile c-d.

Profile h-g runs in an N-S direction perpendicular to the strike of the anomaly. The final best model represents a body with density contrast 340 kg/m^3. The depth to the top of the structure is 0.04 km. The body's width varies increasing with depth, and its depth extent is 3.6 km. The results of modeling the anomaly h-g are shown in Figure 5c.

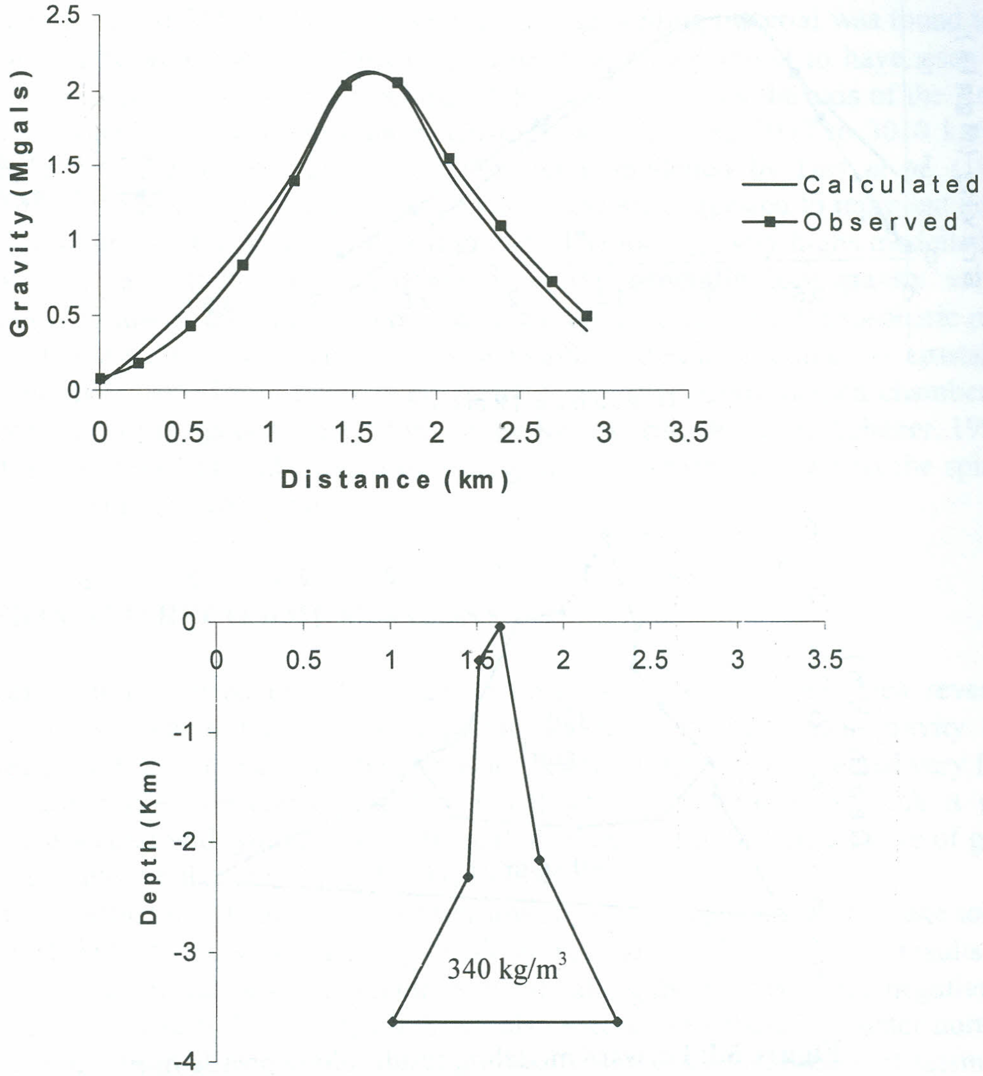

Figure 5c: Forward modeling results along profile h-g.

Profile m-n is oriented in the NNW-SSE direction. The final model is a two-body structure with its parts having density contrasts of 320 and 340 kg/m^3 for its upper and lower parts, respectively. The depth to the top of the body is 0.4 km while it extends to a depth of 6 km. The width of the composite body varies from top to bottom forming a nearly conical shape with a width of about 3 km at the bottom. The results of modeling the anomaly m-n are shown in Figure 5d.

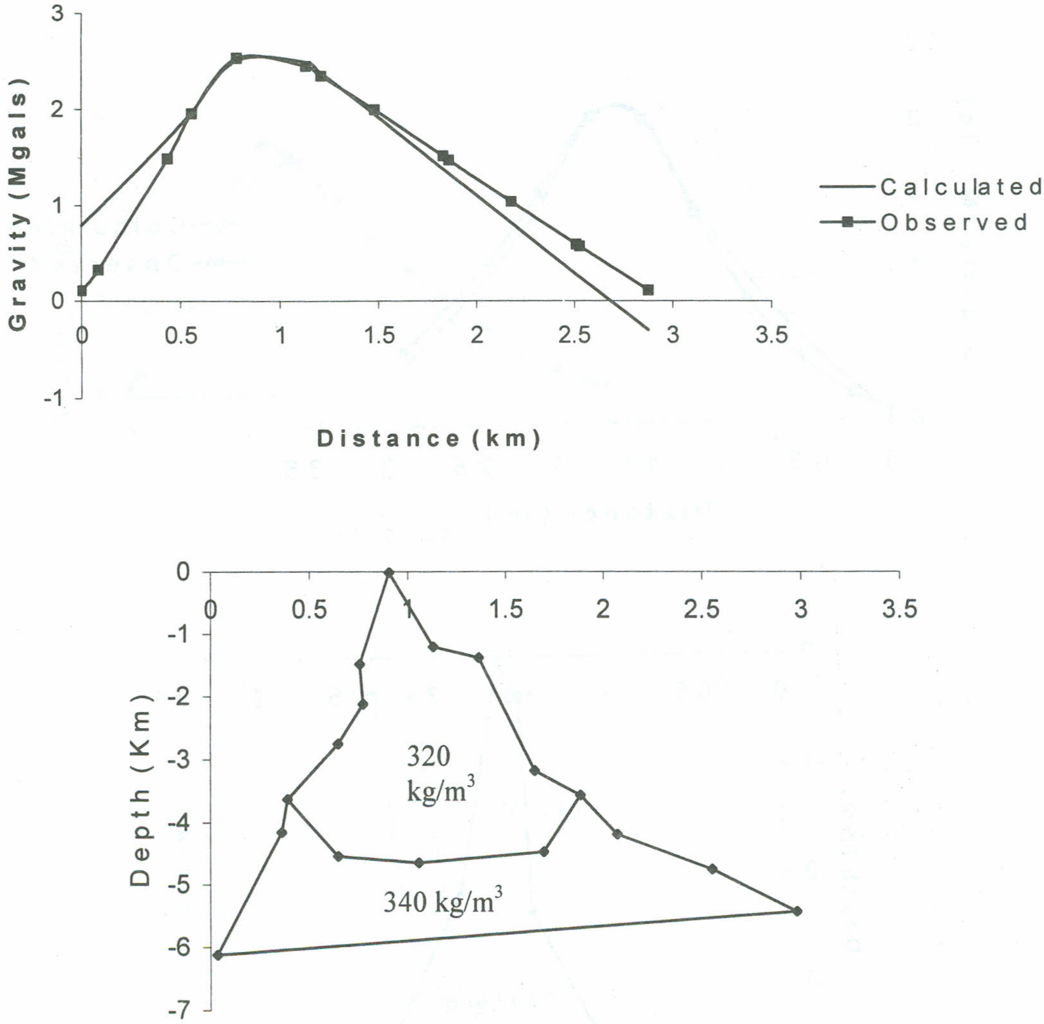

Figure 5d: Forward modeling results along profile m-n.

The Bouguer anomaly map is characterized by a broad gravity low superimposed by positive anomalies. These anomalies are circular and closed, most of them aligned in the NNW-SSE directions. Such circular anomalies are likely to represent high-density intrusives in the relatively low-density graben of the rift. The anomalies along the profile p-q and h-g had been mapped in a previous hydrocarbon exploration project (BEICIP, 1987). The anomalies were not interpreted conclusively since they were considered as local sources irrelevant for that particular study. Githiri *et al.* (2004) from a ground magnetic survey detected had modeled the anomaly along profile p-q as having a magnetization of 1.55 A/M with the bottom of the causative body being at a depth of 1.99 km. This depth to the bottom compares well to the 2 km depth to the bottom of the upper body modeled in this study. The lower part of the causative body along p-q with a density contrast of 290 kg/m^3 may have been at a temperature above Curie point and hence ceasing to be magnetic.

Hay *et al.* (1995), in their gravity model across the rift at the equator, modelled long wavelength components by assigning density contrasts deep in to the mantle. From their results, low mantle density 3000-3150 kg/m^3 representing hot, up welling material was found to occur at a depth of 90 km beneath the East African plateau. It was then found to have risen replacing normal mantle density of 3260 kg/m^3 reaching Moho depths beneath the axis of the Kenyan rift. The intrusives modelled in this study have densities ranging from 2950 to 3010 kg/m^3 which closely compares to the lower mantle density material modelled by Hay *et al.* (1995). The densities of all the bodies vary from 2950-3010 kg/m^3 and are suggested to represent near mantle material that has intruded the Moho at the rift graben. The local gravity highs modelled in all the above profiles in this study are superimposed on the generally low gravity values. This background gravity low is considered to be due to the up doming hot asthenospheric material of less density relative to the lower crust. The near mantle material intruding the crustal rocks as modelled along the selected profiles is likely to have emanated from magma chambers. This is supported by results of the geochemical study of the Kenyan rift, (Ritter & Achauer, 1994) which showed that the origin of crustal magma occurring in a zone extending across the spinel-garnet transition is situated in the upper mantle.

CONCLUSION AND RECOMMENDATIONS

Gravity investigations carried out at the area surrounding Lake Magadi area revealed local anomalies, some of which had not been previously mapped. The local gravity highs are superimposed on low gravity values. The depths to the top of the bodies detected vary from 0.04-0.7 km and are hence considered shallow. Local gravity anomalies in such a geological environment associated with young volcanism and tectonics are usually indicative of geothermal conditions at the intermediate depths (Ndombi, 1978).

The crustal structure of the area has been investigated using local earthquake tomography and spatial distribution of hypocentres by Ibs-Von Seht *et al.* (2001). Their results from the tomography indicate a linear positive velocity anomaly along the rift axis and a negative anomaly at shallow depth underneath Lake Magadi. They also recorded earthquake cluster north of Lake Magadi which comprised 75 per cent of the total observed events with absence of seismic activity below 9 km depth in the area suggesting a lower crustal anomalous body of reduced shear strength. They reported migration of hypocentres from south to north, which may have been due to movement of the earthquake trigger mechanism. Therefore, a detailed gravity survey is recommended in the northern part of the lake, which was not covered in this study to map any anomalous body that may be responsible for earthquakes.

ACKNOWLEDGEMENTS

We wish to acknowledge the Ministry of Energy, University of Nairobi and National Oil Corporation of Kenya for availing facilities and relevant information necessary for this study. We also wish to acknowledge financial support from Kenyatta University.

REFERENCES

Baker, B.H. 1958. Geology of the Magadi area, *Kenya Geological Survey Report. 42*. Government Printers, Nairobi, pp 5–25.

BEICIP, 1987. *Kenya Tertiary Rift Study, Republic of Kenya*, A Report to Ministry of Energy and Regional Development, Nairobi, pp 39–40.

Githiri, J.G., Stangl, R.L., Waithaka, J.W. and Dindi, E.W. 2004. Ground magnetic survey of Magadi geothermal field. *East African Journal of Physical Sciences* 5: 75–78.

Hay, D.E., Wendlandt, R.F. and Keller, G.R. 1995. The origin of Kenya rift plateau-type flood phonolites: Integrated petrologic and geophysical constraints on evolution of the crust and upper mantle beneath the Kenyan Rift. *Journal of Geophysical Research* 100: 10549–10557.

Kearey, P. and Brooks, M. 1984. *An Introduction to Geophysical Exploration*. Blackwell Scientific Publications, London, pp 138–150.

Khan, M.A., Mansfield, J. and Swain, C.J. 1977. *A catalogue of gravity measurements in Kenya*. Geological Department, University of Leicester, London, pp 9–14.

Muiruri, P.N. 1992. *A gravity survey of the Longonot-Suswa Area*. M.Sc. thesis, University of Nairobi, Nairobi, pp 27–82.

Ndolo, J.M. 1989. *Dissertation, geothermal resources of the African Rift Valley with particular reference to Kenya*. Module No. 8364. Oxford Polytechnic, London, pp 8–24.

Ndombi, J.M. 1978. *Geology, gravity and resistivity studies of Olkaria geothermal field*. Ph.D. thesis, University of Stanford, Stanford, pp 42.

Riaroh, D. and Okoth, W. 1994. The geothermal fields of the Kenya rift. *Tectonophysics* 236: 117–130.

Ritter, J.R.R. and Achauer, U. 1994. Crustal tomography of the central Kenya rift. *Tectonophysics* 236: 291–304.

Seht, I.V.M., Blumenstein, S., Wagner, R., Hollnack, D. and Wohlenberg, J. 2001. Seismicity, seismotectonics and crustal structure of the southern Kenya rift - new data from Lake Magadi area. *Geophysical Journal International* 146: 439–453.

Talwani, M., Worzel, J.L. and Landisman, M. 1959. Rapid computation for the two-dimensional bodies with application to the Mendocino submarine fracture zone. *Journal of Geophysical Research* 64: 59.